Catalysis Letters (2019) 149:1415–1426
https://doi.org/10.1007/s10562-019-02724-8

Evaluation of Sodium/Protonated Titanate Nanotubes Catalysts in Virgin and Post Consumer PET Depolymerization

G. R. Lima[1] · W. F. Monteiro[2] · C. M. Scheid[2] · R. A. Ligabue[2] · R. M. C. Santana[1]

Received: 27 November 2018 / Accepted: 19 February 2019 / Published online: 2 March 2019

Abstract

The high PET consume, mainly as bottles, associated with rapid disposal and high resistance to ambient conditions and biological degradation lead to accumulation in the enviromental, constituting a worrying scenario in world level. Chemical recycle PET by glycolysis is an important alternative, once bis(hydroxiethyl)terephthalate (BHET), high added value monomer, can be obtained. In this context, this study approaches the use of titanate nanotubes (*i.e.* sodium/protonated titanate nanotubes) as catalyst for PET glycolysis. Reactional conditions, the origin and granulometry of PET flakes were evaluated (at 196 °C). Best results (BHET yield > 80%) were obtained for both catalyst in 3 h of reaction. The protonated titanate nanotubes catalyst were more efficient than sodium titanate nanotubes due to greater concentration of Brönsted and Lewis acid sites, indicated by TPD analyzes.

Graphical Abstract

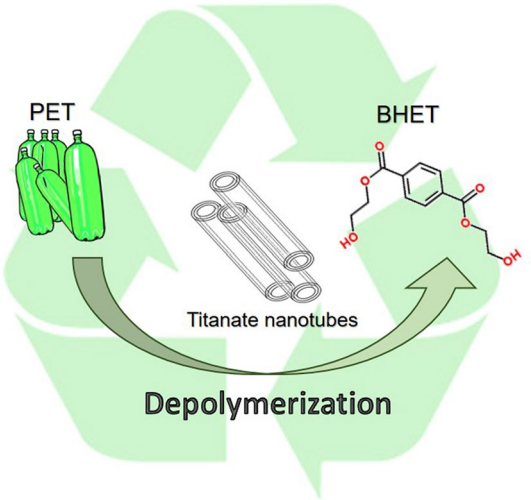

Keywords Chemical recycling · Glycolysis · PET · Nanostructure catalysts · Titanate nanotubes

1 Introduction

Chemical recycling of post-consumer polyethylene terephthalate (PET), a semicrystalline thermoplastic polymer with high added value and very important for global economy due to its wide variety of applications as packaging, fibers, films

G. R. Lima and W. F. Monteiro contributed equally to this work.

Electronic supplementary material The online version of this article (https://doi.org/10.1007/s10562-019-02724-8) contains supplementary material, which is available to authorized users.

✉ R. A. Ligabue
rligabue@pucrs.br

Extended author information available on the last page of the article

among others [1], has received great attention in the field of sustainable technology and resource conservation [2].

In the latest released data, PET consumption in Brazil was estimated to reach 840 kTon in 2016, representing an increase of 12% in relation to 2007, according to data from the Brazilian Association of PET Industry (ABIPET) [3].

The scenary of solids residue in Brazil in 2014, released by the Associação Brasileira de Empresas de Limpeza Pública e Resíduos Especiais (ABRELPE), shows that PET recycling in 2012 represented 58.9%, 1.8% higher than in the previous year [4]. However, in 2015 this dropped to 51% [5], caused by the decrease in the activities of industries that consume recycled raw materials, such as textiles, chemicals and automotive [6], due to the decline in the country's economic activity, which reduces the profitability and consequently the attractiveness of material recycling. The use of PET is mainly on products with a very short shelf life, such as food packaging and bottles, as a result it represents approximately 42% by weight of the fraction referring to the polymers in the urban solid waste, according to the Ciclosoft released by Compromisso Empresarial para Reciclagem (CEMPRE) in 2016 [7]. Moreover, its high resistance to ambient conditions and biological degradation causes the accumulation of this material to be even greater when discarded improperly. In view of the foregoing, PET recycling is an imperative issue.

Among the chemical recycling methods, the most common is glycolysis, in which diols, usually ethylene glycol (EG), are used to break the PET chain bonds and obtain the monomers used in the polymer manufacturing process. The main monomer of this depolymerization is bis (2-hydroxyethyl terephthalate), better known as BHET, which can easily be reintroduced into PET production [8–10].

However, the use of drastic reaction conditions (high time and temperature) leads to research of different metallic catalysts (chlorides, acetates, hydroxides, sulfates, carbonates, among others) that are soluble in ethylene glycol (EG) [9, 11]. Yet some of these catalysts require long reaction time (up to 8 or 9 h) [9, 12] and others achieve a maximum yield of 65%, 50% [13].

In the last decades, the utilization of heterogeneous catalysts has received highlight and their application is explored in different areas as acetalization and ketalization of glycerol [14], epoxidation of olefins [15, 16] conversion of ethanol in 1,3-butadiene [17], as well as, PET glycolysis. The development of catalytic systems based on SO_4^{2-}/ZnO, SO_4^{2-}/TiO_2 and SO_4^{2-}/ZnO-TiO_2 present good performance in the PET glycolysis (PET conversion about 100% and BHET yield about 70%) [18]. The utilization of layered double hydroxides as catalysts showed PET conversion about 100% with BHET yield about 80% [19]. In the context of heterogeneous catalysts, nanostructures emerge as promising materials for areas as biodiesel synthesis [20], CO_2 conversion [21], oxidation of alcohols [22], among others. For PET glycolysis, works that studied Perkalite F100 [23] and γ-Fe_2O_3 [24] reached BHET yield over 80%, however, the reaction conditions used were higher than 240 °C.

Lately, titanate nanotubes (TNT) emerge as a promising material due to their low-cost and synthesis, low toxicity, besides a uniform tubular morphology and high specific surface area (≈ 170 m^2 g^{-1}), making them suitable for surface modification [25, 26]. Between the advantages generated due to high specific surface area of these nanomaterials, there is the large number of acid active sites. Recent studies showed that titanate nanotubes have Brönsted and Lewis acid sites formed from lattice distortion due to the scrolling of titanate nanotubes layers [27]. By hydrothermal method it is possible to obtain TNT with sodium intercalated in its structure (NaTNT). One of the possibilities of modification of this nanostructure is the exchange of Na^+ by H^+, through acid washing resulting in pronotated titanate nanotubes (HTNT). Thus, several studies have shown a range of applications to this nanostructure as catalysts, for example, CO_2 conversion [28], dry reform of methane [29], biodiesel synthesis [30], glycerol acetalization [31], aldol condensation [32] and photocatalysis application [33–35], among others.

In a previous and pioneering work of our group [36], sodium titanate nanotubes (NaTNT) were successfully used as catalysts for the depolymerization of PET by glycolysis. However, the optimal reaction parameters have not been evaluated. In this context, the aims of this work was separated in two step: the first constituting in the evaluation of the influence of PET (virgin and post-consumer) granulometry, EG:PET ratio (w/w) and amount of NaTNT (mol%), as well as, time of reaction. The second step remains an unexplored area consisting in the performance of a comparative study using sodium titanate nanotubes (NaTNT) and protonated titanate nanotubes (HTNT) as catalysts for depolymerization of PET by glycolysis.

2 Materials and Methods

2.1 Materials

The materials used for synthesis of the sodium and protonated titanate nanotubes (NaTNT and HTNT) and glycolysis reactions were: sodium hydroxide (99% Vetec), titanium dioxide (98% anatase phase, JB Química), hydrochloric acid (Anidrol), ethylene glycol (EG, 99.5%, Dinâmica), virgin PET (Rhopet S-80 – Rhodia Ster/ Mossi and Ghisolfi Group) and post-consumer bottle-grade PET. All reactants were used as received.

2.2 Titanate Nanotubes Synthesis

NaTNT were synthesized based on the hydrothermal method [37, 38]. In a beaker was mixed 1.5 g (18.8 mmol) of titanium dioxide and 120 mL of 10 mol L^{-1} NaOH aqueous solution. The mixture was kept under magnetic stirring for 30 min at room temperature. Then the mixture was added to a stainless steel autoclave reactor and remained reacting at 135 ± 5 °C for 72 h. The formed precipitate was centrifuged and washed with distilled water several times until the pH of washing water reached about 7 and dried at 80 °C for 24 h. Protonated titanate nanotubes (HTNT) were obtained from 1.0 g NaTNT (301.7 mol) mixtured with an acid solution (HCl, 0.5 mol L^{-1}) for 30 min at room temperature. After, the precipitate was centrifuged and washed with distilled water several times until the pH of washing water reached about 7 and dried at 80 °C for 6 h.

2.3 PET Glycolysis

For PET glycolysis it was used virgin PET in pellets and post-consumer PET bottles, from carbonated drinks (exclusively of soda) and transparent, in order to avoid variations relating to colorants and the polymer crystallinity. The bodies of PET bottles were washed, dried and grounded with a knife mill in flakes form.

In a typical reaction of PET glycolysis was carried out in a 500 mL round-bottom three-naked flask equipped with magnetic stirrer, thermometer and reflux condenser. The vessel containing the mixture of EG and catalyst was preheated to the selected temperature (196 °C) and, after was added the PET. In all runs 15 g of PET (76.5 mmol) were charged to the reactor. At the end of the reaction, the temperature of the reaction system was reduced to 120 °C. Boiling distilled water (300 mL) was added to the reaction mixture to solubilize the glycolysis product. The mixture was filtered (filter Unifil C42, 1–2 µm) under reduced pressure with a Büchner funnel and the filtrate was stored at 4–10 °C for 72 h to form BHET crystals. After, BHET crystals were filtered (G4 sintered glass funnel and filter Unifil C42, 1–2 µm) under. Lastly, the white BHET crystals were dried at 60 °C for 24 h and weighted in an analytical balance to estimate the BHET yield (Y) according to Eq. (1):

$$Y = \frac{W_{BHET,f} / MW_{BHET}}{W_{PET,i} / MW_{PET}} \times 100, \quad (1)$$

where $W_{BHET,f}$ represents the final weight of BHET, MW_{BHET} represents the molar weight of BHET (254 g mol^{-1}), $W_{PET,i}$ represents the initial weight of PET used in the reaction and MW_{PET} represents the molecular weight of the repeat unit of PET chain (192 g mol^{-1}).

The conversion (C) of PET in glycolysis reactions was calculated based on Eq. (2):

$$C = \frac{W_i - W_f}{W_i} \times 100, \quad (2)$$

where W_i represents the initial weight of PET and W_f represents the weight of undepolymerized PET. All reactions were performed in duplicate and the experimental error of about 3% was accepted.

2.3.1 Effect of Granulometry of Post-consumer PET in PET Glycolysis

The comminution process of post-consumer PET bottles produces flakes of different sizes, which were separated as follows: particles from 1.00 to 2.36 mm (granulometry 1), particles from 2.36 to 4.75 mm (granulometry 2) and particles larger than 4.75 mm (granulometry 3) using AAKER sieves with 16 mesh opening and KAMACHA with 8 and 4 mesh opening. These three different grain sizes were used in the post-consumer PET depolymerization reaction by glycolysis to evaluate the influence of particle size. All reactions were realized up to 4 h.

2.3.2 Effect of EG:PET Weight and PET:Catalyst mol% Ratio in PET Glycolysis

Table 1 summarizes the experimental conditions to all runs carried out in this part of the work. The EG:PET weight ratio varied between 2:1 and 8:1. NaTNT was used as catalyst in all runs and the catalyst content (relative to the amount of

Table 1 Reactional parameters of the glycolysis reactions carried out for PET:EG weight ratio and content of NaTNT (mol%) study in this work

Run*	PET type	EG:PET (w/w)	NaTNT (mol%)
1	Virgin	2:1	1
2	Virgin	4:1	1
3	Virgin	6:1	1
4	Virgin	8:1	1
5	Virgin	4:1	2
6	Virgin	4:1	3
7	Virgin	4:1	6
8	Post-consumer	2:1	1
9	Post-consumer	4:1	1
10	Post-consumer	6:1	1
11	Post-consumer	8:1	1
12	Post-consumer	4:1	2
13	Post-consumer	4:1	3
14	Post-consumer	4:1	6

PET used) in mol% varied between 1 and 6. All reactions were realized up to 4 h.

2.4 Characterization

2.4.1 Transmission Electron Microscopy (TEM)

The evaluation of the internal structure and numbers of rolled multilayer lamellar walls of TNT was made using transmission electron microscopy (FEI Tecnai G2 T20) using cupper grids with carbon film (300 mesh). The measures of TNT dimensions were obtained by FESEM analysis used Image *J* software (number of measurements = 25).

2.4.2 X-Ray Diffraction (XRD)

The characterization of the crystalline structure of TNT was made by X-ray diffraction analysis (Shimadzu XRD 7000) using radiation K_α of the copper ($\lambda = 1.542$ Å), voltage 40 kV, 30 mA, scanning between 5°–70° 2θ, scan speed of 0.02° and counting time of 2.0 s. In all analysis TNT was in powder form.

2.4.3 Temperature Program Desorption (TPD)

TPD analyzes were performed in a multipurpose system (SAMP3). The sample were first degassed at 100 °C in He flow (30 min) and then saturated with 5% NH_3 or 30% CO_2 in He (v/v) for TPD-NH_3 and TPD-CO_2, respectively. After adsorption, the sample were purged in pure He flow for 30 min to remove physosorbed/weakly adsorbed species, and then heating was initiated at the rate of 10 °C min^{-1} in 30 mL min^{-1} of He flow. Desorption curves were recorded using a thermal conductivity detector (TCD).

2.4.4 Differential Scanning Calorimetry (DSC)

BHET formed by PET depolymerization reactions were characterized by thermal analysis of Differential Scanning Calorimetry (DSC) in a calorimeter, Model Q20 from TA Instruments in the range from 45 to 270 °C at a heating rate of 10 °C min^{-1}, under inert atmosphere of N_2.

2.4.5 Thermogravimetric Analysis (TGA)

The thermal stability of starting virgin and post-consumer PET and BHET formed by PET depolymerization reactions were characterized by thermogravimetric analysis (TGA) in a SDT equipment, Model Q600 from TA Instruments in the range from 50 to 800 °C at a heating rate 20 °C min^{-1}, under inert atmosphere of N_2.

2.4.6 Nuclear Magnetic Resonance Spectroscopy (NMR)

In order to confirm the production of BHET, ^{1}H-NMR and ^{13}C-NMR were recorded on a Bruker Ascend 400 NMR spectrometer operating at 400 MHz in deuterated DMSO solution.

3 Results and Discussion

3.1 Effect of Granulometry of Post-consumer PET in PET Glycolysis

In order to evaluate the influence of post-consumer PET granulometry in the BHET formation, thermal analyses by DSC for the glycolysis reactions of PET using different particle sizes were performed and the results are presented in Fig. 1. The behavior of the curves is quite similar, showing that the reactions presented BHET yields without residual PET. A strong endothermic peak located at about 110 °C corresponding to the BHET melting temperature [39] is displayed for all samples. Considering that none PET flakes remain in the first filtration, can be concluded that PET conversion was about 100%. In the DSC results, no peaks corresponding to dimers and oligomers (165 °C) [40] are presented showing high purity of product. The weak signal between 200 and 230 °C can be associated to BHET polycondensation [41].

The yield values (Y) in BHET are presented in Table 2. As observed, the results are similar for all granulometries, considering the estimate error (≈3%). In general, the highest BHET yields were obtained with smaller pellets of PET in 3 h of reaction (1.00–2.36 mm), because there was an increase in the available surface area for the reaction to occur [42, 43]. Maximum yields values for granolumetry

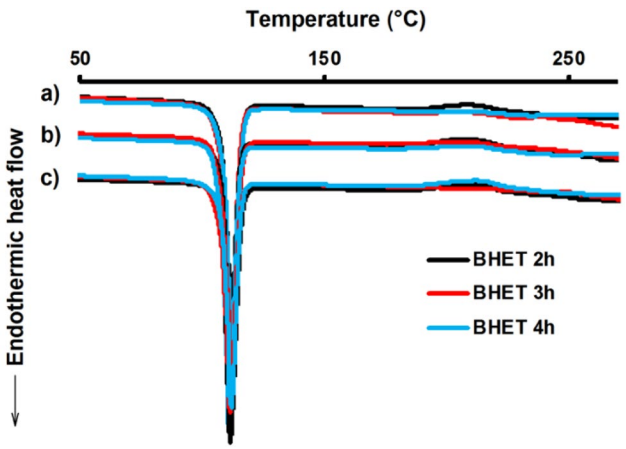

Fig. 1 Comparative DSC curves of BHET from PET granulometry: *a* 1 (1.00–2.36 mm), *b* 2 (2.36–4.75 mm) and *c* 3 (larger than 4.75 mm)

Table 2 Results of BHET yield (Y, %) for different times and granulometries

PET granulometry (mm)	Time (h)	Y (%)
1 (1.00–2.36)	2	67
	3	80
	4	78
2 (2.36–4.75)	2	57
	3	76
	4	60
3 (>4.75)	2	70
	3	71
	4	77

1 and 2 were obtained with 3 h reaction time (80 and 76%, respectively).

To decreasing trend on yield value for 4 h reaction time may be an indicative that the glycolysis has reached the reaction equilibrium, since the depolymerization of PET can be considered a reversible reaction [42]. For grain sizes larger than 4.75 mm, the better result was obtained with 4 h of reaction.

3.2 Effect of Reaction Parameters in PET Glycolysis

Since the BHET yield results obtained with post-consumer PET using granulometry 1 (1.00–2.36) were superior (80% in 3 h of reaction), this granulometry was chosen to be used in the others stages of the study. Figure 2 shows the influence of the EG:PET weight ratio and NaTNT content (mol%), for both virgin and post-consumer PET (runs 1–14, Table 1) to 4 h of reaction. This time was chosen to evaluate the possibility of repolymerization once the equilibrium is achieved in 3 h. As observed in Fig. 2a, with the increase of EG:PET ratio, there is also an increase on BHET yield. Above EG:PET of 4:1 there is no significant difference on BHET yield, with values close to 80% similar to that found by López-Fonseca et al. using zinc and sodium compounds as catalysts [13]. This result shows that it is not necessary to use a large excess of ethylene glycol in the depolymerization of both PET.

When evaluating the effect of NaTNT content (mol%, EG:PET 4:1, 4 h of reaction, Fig. 2b), there is a more significant difference the higher the percentage of the catalyst used. For virgin PET, the BHET yield remains constant up to 2 mol% catalyst. However, the use of larger contents leads a decrease of up to 20%. On the other hand, for post-consumer PET, 1 mol% of catalyst has the highest BHET yield value, dropping from approximately 20% to 2, 3 and 6 mol%. This decrease in yield with higher catalyst contents may be associated with the agglomeration of nanostructures, which is increased with high catalyst concentrations, decreasing the

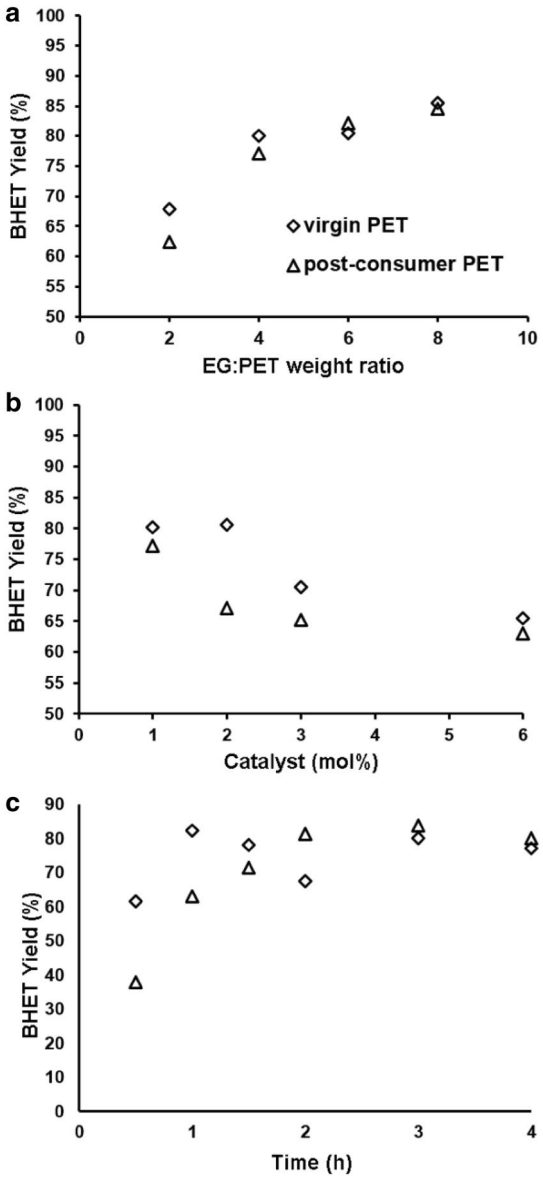

Fig. 2 Effect of **a** EG:PET weight ratio, **b** NaTNT content (mol%) and **c** reaction time on BHET yield for virgin and post-consumer PET

accessibility of the active sites [44], or even the reversibility of the reaction (BHET polycondensation) leading dimer, trimers or oligomers products [45].

Evaluation of influence of reaction time in BHET yield is presented in Fig. 2c, where the EG:PET weight ratio of 4:1 and amount of catalysts of 1% in relation to PET were used. For both virgin and post-consumer PET, the reaction equilibrium is reach between 3 and 4 h of reaction. In 0.5 h of reaction, the BHET yields reach 65% and 38% using virgin and post-consumer PET, respectively.

DSC and TG curves of BHET are presented in Fig. 3. These results are related to some conditions adopted (4:1 EG:PET, 1 mol% of catalyst and 4 h). The other conditions

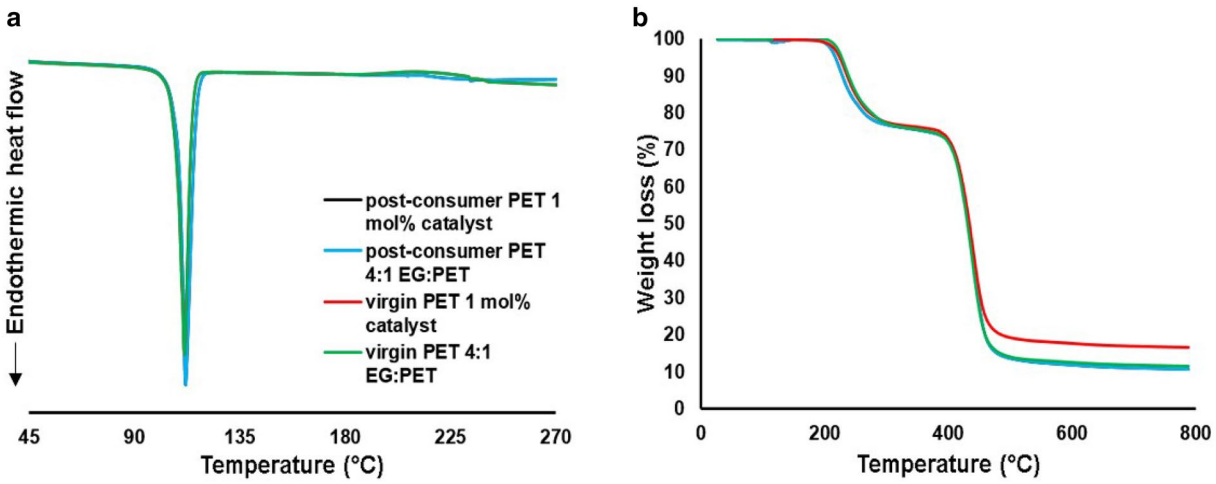

Fig. 3 **a** DSC and **b** TG curves of BHET with for different reactions conditions for virgin and post-consumer PET

are presented in supplementary material. It is observed in DSC curves that there was BHET formation, confirmed by the endothermic peak at about 110 °C [46]. Moreover, there are not observed peaks corresponding to dimers or oligomers (~ 170 °C) [42] and unreacted PET (255–265 °C) [47]. TG curves of BHET exhibit two steps of weight losses. The first one, between 200 and 300 °C, shows approximately 20% and refers to BHET thermal decomposition [36]. The second occurs between 300 and 550 °C with about 65% of weight loss and is attributed to thermal degradation of PET produced by the thermal polymerization of BHET during the thermogravimetric analysis process [48]. The residues to all analysis are approximately 15%.

BHET samples were also analyzed by ^{1}H-NMR and ^{13}C-NMR to prove its chemical structure. ^{1}H-NMR and ^{13}C-NMR spectra are shown in Fig. 4, along with an illustration of the chemical structure of the compound.

In ^{1}H-NMR spectrum, the signals labelled as 1, 2, 3 and 4 (Fig. 4a) are attributed to protons of the aromatic ring ($\delta_H = 8.11$ ppm, s, 4H), hydroxyl groups ($\delta_H = 4.96$ ppm, t, 2H), methylenes (–CH_2–) adjacent to –OH groups ($\delta_H = 3.53$ ppm, m, 4H), methylenes (–CH_2–) adjacent to –COO groups ($\delta_H = 4.33$ ppm, t, 4H), respectively. Signal in 2.5 ppm is DMSO and in 3.3 can be attributed to residual H_2O [10, 47]. In ^{13}C-NMR spectrum, the signals labelled as 1 ($\delta_C = 165.55$ ppm), 2 ($\delta_C = 134.15$ ppm),

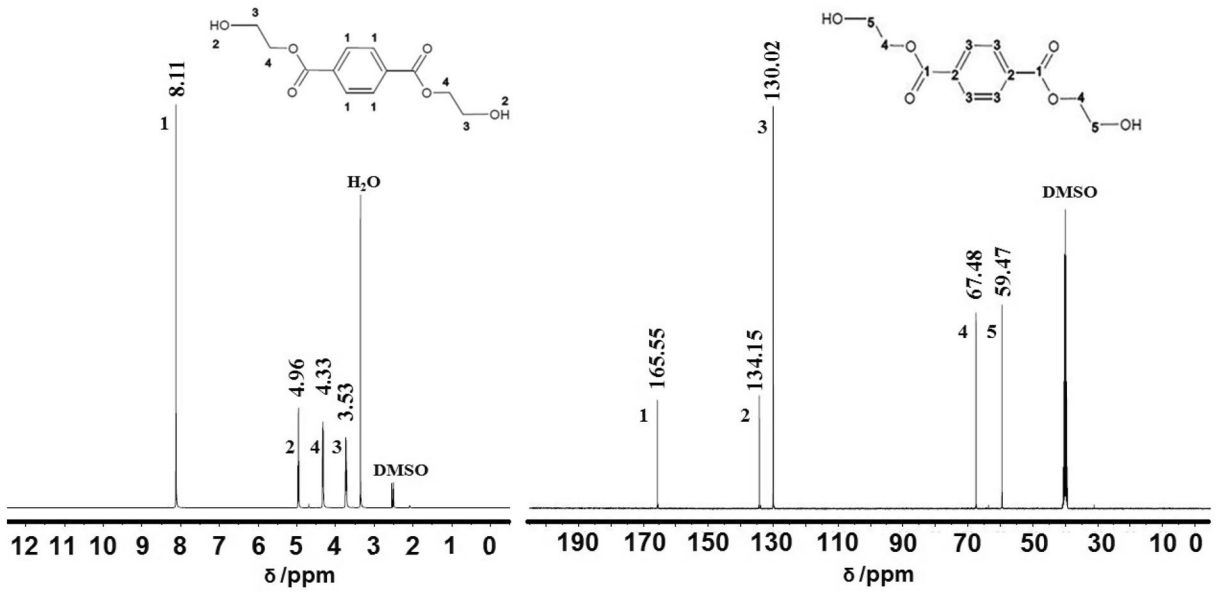

Fig. 4 **a** ^{1}H-NMR and **b** ^{13}C-NMR spectra of BHET obtained from post-consumer PET with the use of NaTNT for 4 h reaction

3 ($\delta_C = 130.02$ ppm), 4 ($\delta_C = 67.48$ ppm) and 5 ($\delta_C = 59.47$ ppm) are attributed to carbons of the BHET chemical structure, as shown in Fig. 4b. DMSO signal appears in 40 ppm.

3.3 Comparative Study Between NaTNT and HTNT as Catalysts

NaTNT has ability to make ion exchange with a diverse ions range, among them, the H^+ ions are inserted into the structure by a simple acid washing process. In this way, a protonated nanostructure (HTNT) was obtained and characterized. Figure 5 presents the results obtained by TEM analysis, in which NaTNT and HTNT nanostructures have a similar tubular morphology, but with difference in external diameter being 8.8 ± 0.8 nm to NaTNT and 10.4 ± 0.8 nm to HTNT (calculated using Image *J* software in Fig. 5). Besides that, its observed that NaTNT presented a tubular morphology more defined, making possible the visualization of internal walls, while HTNT presented a roughness in the surface and a lower crystallinity similar to find in the literature [50, 51].

Figure 6 shows the XRD and Raman results obtained for NaTNT and HTNT nanostructures. The first one has a monoclinic structure belonging to the space group P21/m showing diffraction peaks located at $2\theta = 10°$, 24°, 28°, 48° and 61°. In addition, a low intensity peak is observed at 62° due to the intercalation of the Na^+ ions between the lamellae. The peak located at 10° refers to the interlamellar distance of the structure being equal to 0.87 nm. The ion exchange promoted a reduction in the crystallinity observed by the decrease in the intensity of the peak located at $2\theta = 10°$, suggesting the structure $H_2Ti_3O_7$, belonging to the space group C2/m, similar to literature [31, 52]. Furthermore, the low peak intensity compared to the 28° peak at 24° shows that the ion exchange of Na^+ by H^+ cations was successfully achieved [53]. Interlamelar distance to HTNT is 0.92 nm,

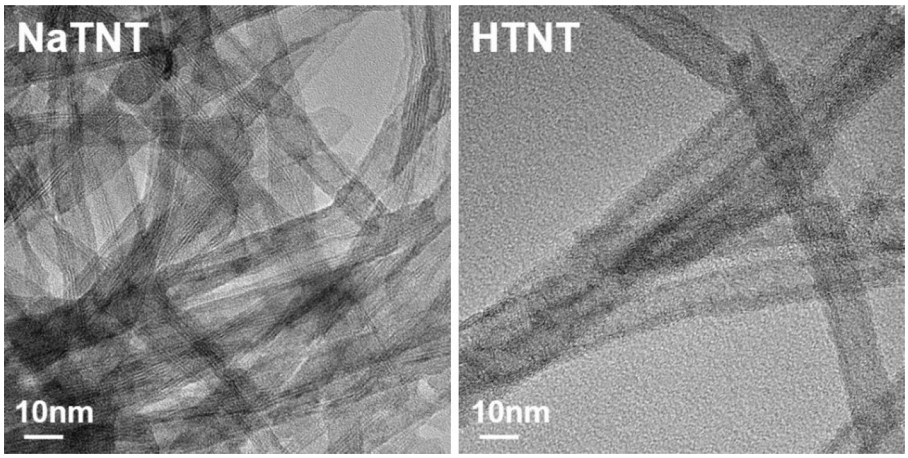

Fig. 5 TEM micrographs of NaTNT and HTNT catalysts

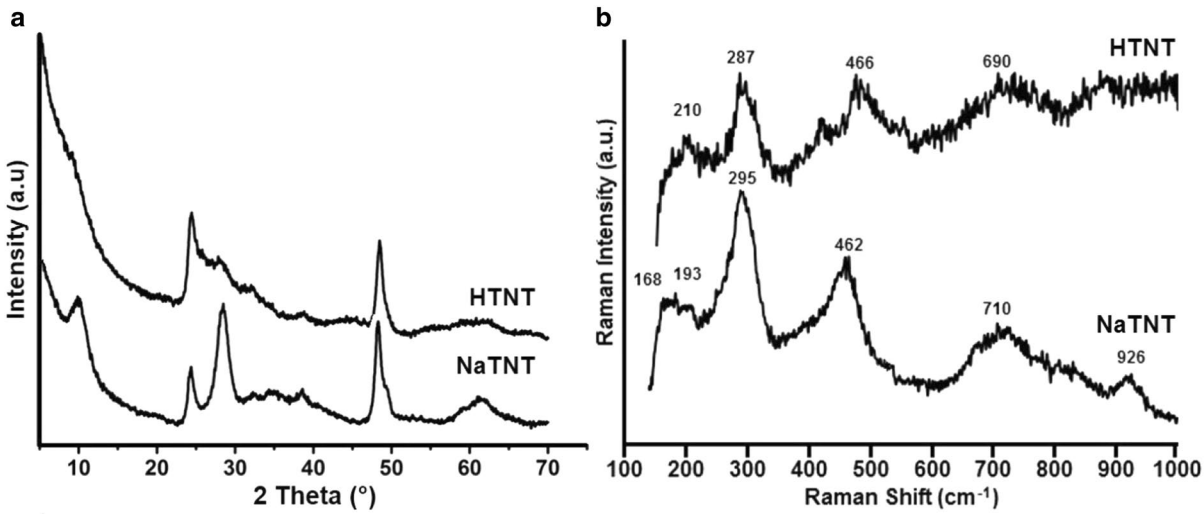

Fig. 6 **a** XRD and **b** Raman of NaTNT and HTNT catalysts

this increase being due to the addiction of H_3O^+ ions [31]. Raman results of NaTNT present bands at about 168 and 193 that are attributed to the Na···O–Ti bending modes [54]. Bands around at 295, 462, 710 and 926 cm^{-1} are assigned to the Ti–O–Ti stretching vibration from the TiO_6 octahedra from edge-shared TiO_6 [54, 55]. Similarly, Raman spectrum of HTNT shows the same characteristics bands of titanate phase. However the absence of band in 926 cm^{-1} indicating the efficiency of ion exchange. These results are in agreement with those of the literature [31, 55, 56].

In order to evaluate the influence of the cation exchange of Na^+ by H^+ on the active sites of the nanostructures, TPD analyzes for NH_3 and CO_2 were performed, shown in Fig. 7. Desorption of NH_3 or CO_2 are observed three distinct regions located in peaks between 130 and 200 °C, 250–300 °C and 320–400 °C assigned to the weak, medium and strong sites, respectively. The total acid sites quantification was 0.34 and 0.79 mmol NH_3 g^{-1} for the NaTNT and HTNT, respectively, while the values obtained for total basic sites were 0.20 and 0.35 mmol CO_2 g^{-1}, for the NaTNT and HTNT nanostructures, respectively. This result are in according with literature [57] indicating a more acidic character in these catalysts and showing that the HTNT nanostructure presents more active sites.

In order to compare the two catalysts, NaTNT and HTNT, were performed glycolysis reactions using virgin and post-consumer PET (particle size 1.00–2.36 mm) at 2, 3 and 4 h (Fig. 8). In all reactions the conversion of PET was about 100%. For virgin PET, in 3 h of reaction the HTNT showed to be a slightly more effective than NaTNT with BHET yields of 88 and 84%, respectively. Whereas for the time of 4 h the effect of repolymerization becomes expressive, decreasing its yield in BHET to 80% and 76% for NaTNT and HTNT, respectively. When using post-consumer PET, HTNT nanostructure is more effective in the three reaction

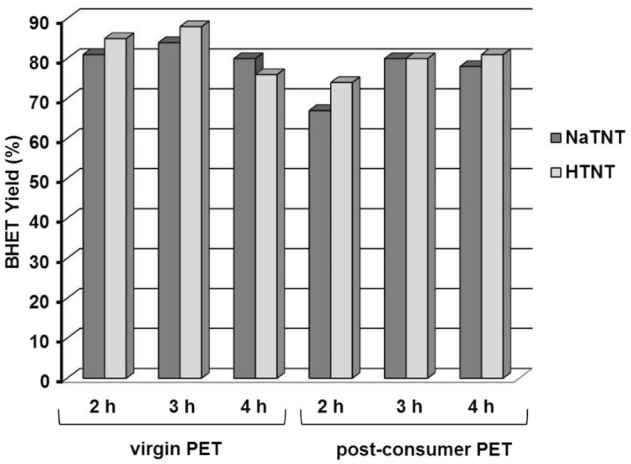

Fig. 8 Results of BHET yield (%) in function of glycolysis reaction time using virgin and post-consumer evaluating NaTNT and HTNT as catalyst

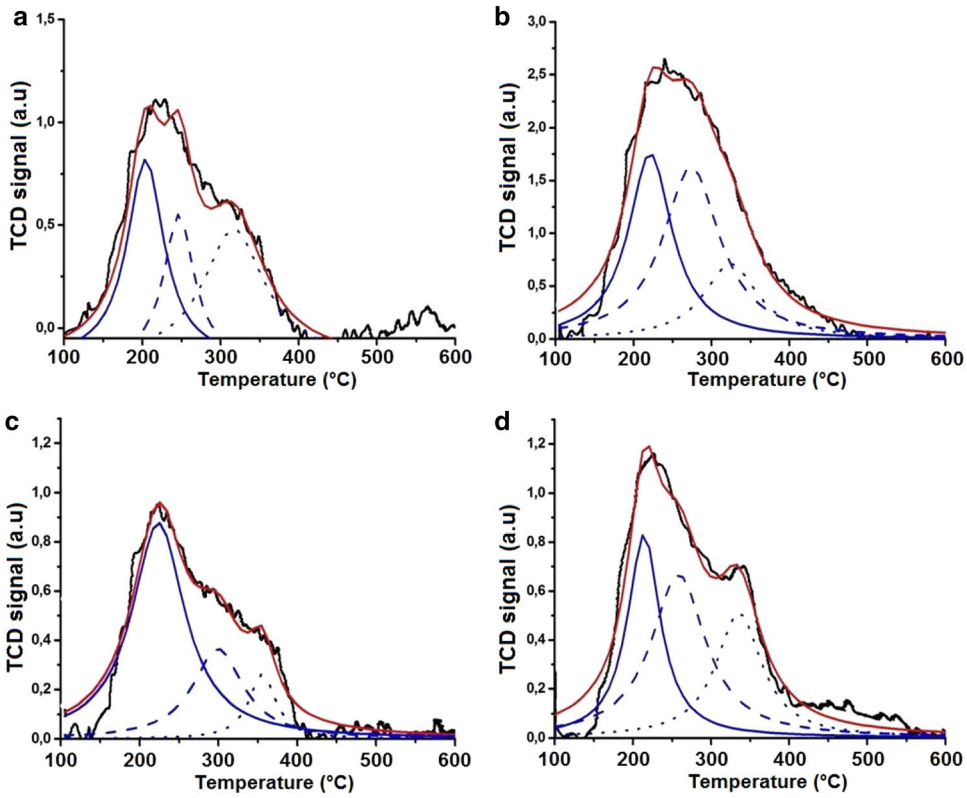

Fig. 7 NH_3-TPD results for **a** NaTNT and **b** HTNT. CO_2-TPD results for **c** NaTNT and **d** HTNT. The blue curves corresponding to curve fitting of weak (line), medium (dash line) and strong (dot line) sites

times evaluated, showing BHET yields equal to 74 and 81%, respectively, whereas NaTNT presented values at 67 and 78%, for 2 and 4 h, respectively.

These better catalytic activity of HTNT are in accordance to value obtained by TPD analyzes. More acid actives sites present in the surface made this catalyst more promisor for PET glycolysis. The proposed mechanism of TNT-catalyzed PET glycolysis is illustrated in Fig. 9. PET glycolysis reaction can occur through the acyl-type mechanism ($A_{AC}2$) according to literature [49]. TNTs catalysts present both Brönsted and Lewis sites in their structure. It is suggested that the specie that would be formed ($Ti_3O_7^{2-}$), a Brönsted base, can deprotonate the ethylene glycol, making it a better nucleophile, specie (1). Lewis acid sites (Na^+ or H^+ ions) can form an electron donor–acceptor specie (2) with the carbonyl oxygen of the PET chain (Step 1). Thus, the oxygen of the hydroxyl group of EG has a higher nucleophilicity to attack the carbonyl carbon of the PET chain leading a concerted (Step 2). This step leads the break of PET chain producing two smaller chains and regenerating the catalyst (Step 3) [19, 58]. The new chains return to the catalytic cycle lead to formation of oligomers, dimers and BHET. The high catalytic activity of TNTs in conversion of PET to BHET may be due to the fact that the acidic and basic sites of TNT may act concomitantly in the depolymerization mechanism of PET.

4 Conclusions

The reaction parameters evaluated with the use of sodium titanate nanotubes as a catalyst, such as PET granulometry, EG: PET ratio (w/w) and molar percentage of TNT (mol%) had no influence on BHET purity, interfering only with yield

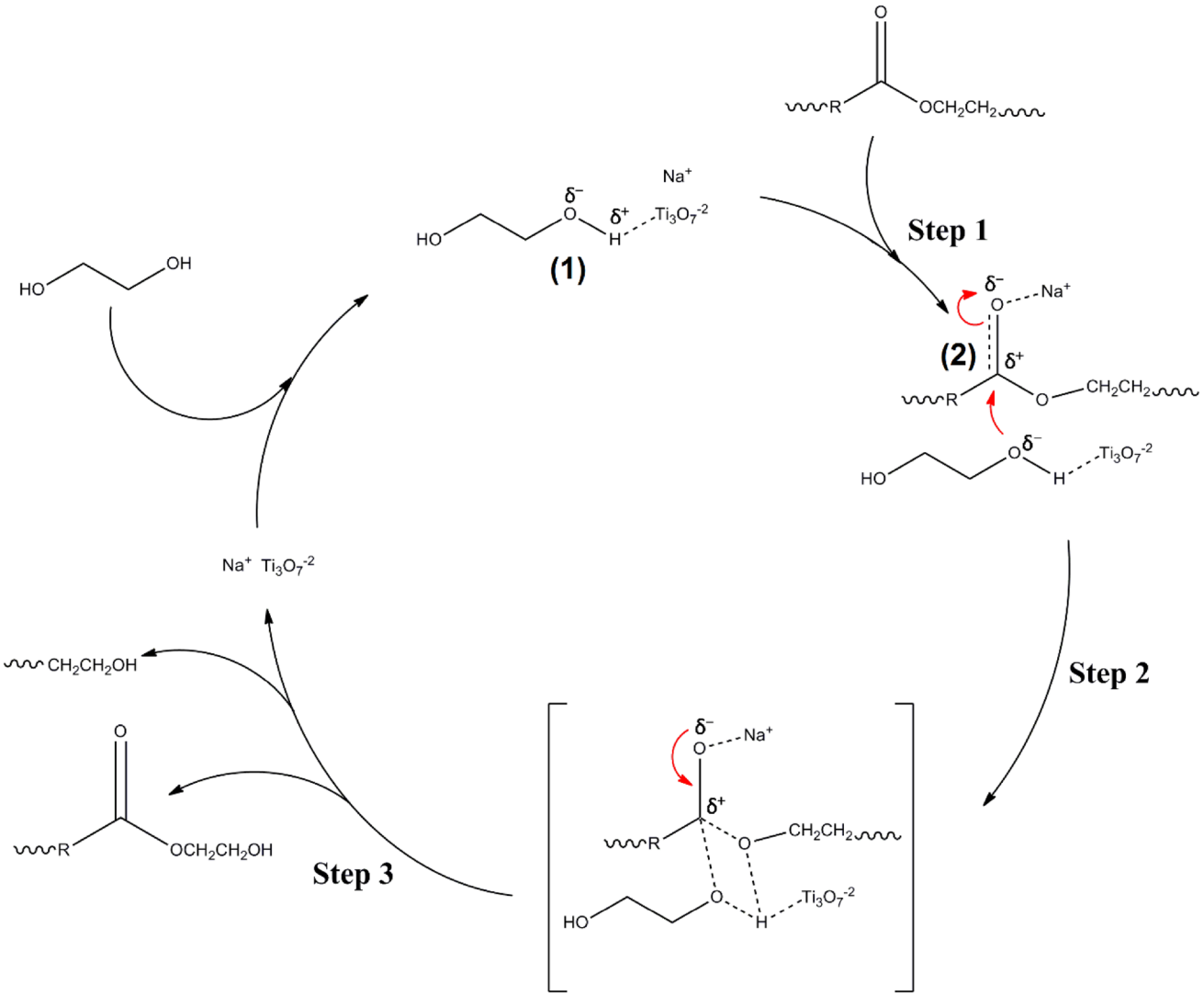

Fig. 9 Proposed mechanism of PET glycolysis catalyzed by NaTNT and HTNT

values. The best granulometry, among those studied, is of 1.00–2.36 mm, presenting higher yields in relation to the others in 3 h of reaction. For the EG:PET ratios, the best relation yield/amount of ethylene glycol used was obtained in 4:1. The most efficient percentage of TNT was 1 mol%, yielding approximately 80%. HTNT presented as a more promising catalyst than NaTNT for PET glycolysis, with a maximum yield of 88% compared to 84% when using NaTNT at 3 h depolimerization of virgin PET. The use of HTNTs maintained the purity of the product obtained, confirmed by DSC and TGA analyzes. Thus, this study shows that NaTNT and HTNT are efficient catalysts for the depolymerization of PET by glycolysis, presenting high yields.

Acknowledgements This study was financed in part by the Coordenação de Aperfeiçoamento de Pessoal de Nivel Superior – Brasil (CAPES) – Finance Code 001. The authors thank CNPq and CAPES by scholarships. PUCRS and UFRGS for technical support: the Laboratório Central de Microscopia e Microanálise (LabCEMM/PUCRS) by morphological analyzes, the Prof. Dr. Oscar W. Perez Lopez and the Laboratório de Processos Catalíticos (PROCAT/UFRGS) by TPD analyzes.

References

1. Dang Y, Luo X, Wang F, Li Y (2016) Waste Manag 52:360–366
2. Sangalang A, Bartolome L, Kim DH (2015) Polym Degrad Stab 115:45–53
3. ABIPET (2013) Indústria do PET no Brasil: Mercados, perspectivas e reciclagem (Panorama 2013). http://www.abipet.org.br/index.html?method=mostrarInstitucional&id=36. Accessed 23 Aug 2018
4. ABRELPE (2014) Panorama dos Resíduos Sólidos No Brasil. http://www.abrelpe.org.br/panorama_apresentacao.cfm. Accessed 22 Aug 2018
5. ABRELPE (2015–2016) Panorama dos Resíduos Sólidos no Brasil. http://www.abrelpe.org.br/panorama_apresentacao.cfm. Accessed 22 Aug 2018
6. ABIPET (2014) Censo da Reciclagem de PET no Brasil – 10a Edição. http://www.abipet.org.br/index.html?method=mostrarDownloads&categoria.id=3. Accessed 4 Sept 2018
7. CEMPRE (2016) Ciclosoft—2016. http://cempre.org.br/ciclosoft/id/8. Accessed 4 Sept 2018
8. Wang H, Liu Y, Li Z et al (2009) Glycolysis of poly(ethylene terephthalate) catalyzed by ionic liquids. Eur Polym J 45:1535–1544. https://doi.org/10.1016/j.eurpolymj.2009.01.025
9. Imran M, Kim DH, Al-Masry WA et al (2013) Manganese-, cobalt-, and zinc-based mixed-oxide spinels as novel catalysts for the chemical recycling of poly(ethylene terephthalate) via glycolysis. Polym Degrad Stab 98:904–915. https://doi.org/10.1016/j.polymdegradstab.2013.01.007
10. Viana ME, Riul A, Carvalho GM et al (2011) Chemical recycling of PET by catalyzed glycolysis: kinetics of the heterogeneous reaction. Chem Eng J 173:210–219. https://doi.org/10.1016/j.cej.2011.07.031
11. Fang P, Liu B, Xu J et al (2018) High-efficiency glycolysis of poly(ethylene terephthalate) by sandwich-structure polyoxometalate catalyst with two active sites. Polym Degrad Stab 156:22–31. https://doi.org/10.1016/j.polymdegradstab.2018.07.004
12. Shukla SR, Kulkarni KS (2002) Depolymerization of poly(ethylene terephthalate) waste. J Appl Polym Sci 85:1765–1770. https://doi.org/10.1002/app.10714
13. López-Fonseca R, Duque-Ingunza I, de Rivas B et al (2010) Chemical recycling of post-consumer PET wastes by glycolysis in the presence of metal salts. Polym Degrad Stab 95:1022–1028. https://doi.org/10.1016/j.polymdegradstab.2010.03.007
14. Manjunathan P, Marakatti VS, Chandra P et al (2018) Mesoporous tin oxide: an efficient catalyst with versatile applications in acid and oxidation catalysis. Catal Today 309:61–76. https://doi.org/10.1016/j.cattod.2017.10.009
15. Masteri-Farahani M, Mirshekar S (2018) Covalent functionalization of graphene oxide with molybdenum-carboxylate complexes: new reusable catalysts for the epoxidation of olefins. Colloids Surfaces A Physicochem Eng Asp 538:387–392. https://doi.org/10.1016/j.colsurfa.2017.11.025
16. Abou Khalil T, Boujday S, Blanchard J, Bergaoui L (2018) Characterization and catalytic activity of Mn(salen) supported on a silica/clay-mineral composite: influence of the complex/support interaction on the catalytic efficiency. Chem Afr 1–11. https://doi.org/10.1007/s42250-018-0023-7
17. Akiyama S, Miyaji A, Hayashi Y et al (2018) Selective conversion of ethanol to 1,3-butadiene using germanium talc as catalyst. J Catal 359:184–197. https://doi.org/10.1016/j.jcat.2018.01.001
18. Zhu M, Li S, Li Z et al (2012) Investigation of solid catalysts for glycolysis of polyethylene terephthalate. Chem Eng J 185–186:168–177. https://doi.org/10.1016/j.cej.2012.01.068
19. Eshaq G, Elmetwally AE (2016) Mg–Zn–Al layered double hydroxide as a regenerable catalyst for the catalytic glycolysis of polyethylene terephthalate. J Mol Liq 214:1–6. https://doi.org/10.1016/j.molliq.2015.11.049
20. Kaur M, Malhotra R, Ali A (2018) Tungsten supported Ti/SiO_2 nanoflowers as reusable heterogeneous catalyst for biodiesel production. Renew Energy 116:109–119. https://doi.org/10.1016/j.renene.2017.09.065
21. Lin YF, Huang KW, Ko BT, Lin KYA (2017) Bifunctional ZIF-78 heterogeneous catalyst with dual Lewis acidic and basic sites for carbon dioxide fixation via cyclic carbonate synthesis. J CO2 Util 22:178–183. https://doi.org/10.1016/j.jcou.2017.10.005
22. Sun Y, Cao C, Wei F et al (2016) Nanocarbon-based TEMPO as stable heterogeneous catalysts for partial oxidation of alcohols. Sci Bull 61:772–777. https://doi.org/10.1007/s11434-016-1070-6
23. Guo Z, Lindqvist K, de la Motte H (2018) An efficient recycling process of glycolysis of PET in the presence of a sustainable nanocatalyst. J Appl Polym Sci 135:6–11. https://doi.org/10.1002/app.46285
24. Bartolome L, Imran M, Lee KG et al (2014) Superparamagnetic γ-Fe_2O_3 nanoparticles as an easily recoverable catalyst for the chemical recycling of PET. Green Chem 16:279–286. https://doi.org/10.1039/C3GC41834K
25. Sallem F, Chassagnon R, Megriche A et al (2017) Effect of mechanical stirring and temperature on dynamic hydrothermal synthesis of titanate nanotubes. J Alloys Compd 722:785–796. https://doi.org/10.1016/j.jallcom.2017.06.172
26. Monteiro WF, Santos CAB, Hoffmann MS et al (2018) Modified titanate nanotubes for the production of novel aliphatic polyurethane nanocomposites. Polym Compos 1–9. https://doi.org/10.1002/pc.25038
27. Camposeco R, Castillo S, Mejia-Centeno I et al (2016) Behavior of Lewis and Brönsted surface acidity featured by Ag, Au, Ce, La, Fe, Mn, Pd, Pt, V and W decorated on protonated titanate nanotubes. Microporous Mesoporous Mater 236:235–243. https://doi.org/10.1016/j.micromeso.2016.08.033
28. Monteiro WF, Vieira MO, Aquino AS et al (2017) CO_2 conversion to propylene carbonate catalyzed by ionic liquid containing

organosilane groups supported on titanate nanotubes/nanowires. Appl Catal A 544:46–54. https://doi.org/10.1016/j.apcata.2017.07.011
29. Coelho DC, Oliveira AC, Filho JM et al (2016) Effect of the active metal on the catalytic activity of the titanate nanotubes for dry reforming of methane. Chem Eng J 290:438–453. https://doi.org/10.1016/j.cej.2016.01.051
30. Hernández-Hipólito P, García-Castillejos M, Martínez-Klimova E et al (2014) Biodiesel production with nanotubular sodium titanate as a catalyst. Catal Today 220–222:4–11. https://doi.org/10.1557/adv.2015.52
31. de Carvalho DC, Oliveira AC, Ferreira OP et al (2017) Titanate nanotubes as acid catalysts for acetalization of glycerol with acetone: Influence of the synthesis time and the role of structure on the catalytic performance. Chem Eng J 313:1454–1467. https://doi.org/10.1016/j.cej.2016.11.047
32. Sluban M, Bogdan C, Parvulescu VI et al (2017) Protonated titanate nanotubes as solid acid catalyst for aldol condensation. J Catal 346:161–169. https://doi.org/10.1021/ja100435w
33. László B, Baán K, Varga E et al (2016) Photo-induced reactions in the CO_2-methane system on titanate nanotubes modified with Au and Rh nanoparticles. Appl Catal B Environ 199:473–484. https://doi.org/10.1016/j.apcatb.2016.06.057
34. Aouadi I, Touati H, Tatibouët JM, Bergaoui L (2017) Titanate nanotubes as ethanol decomposition catalysts: effect of coupling photocatalysis with non-thermal plasma. J Photochem Photobiol A 346:485–492. https://doi.org/10.1016/j.jphotochem.2017.06.030
35. Kiatkittipong K, Assabumrungrat S (2017) A comparative study of sodium/hydrogen titanate nanotubes/nanoribbons on destruction of recalcitrant compounds and sedimentation. J Clean Prod 148:905–914. https://doi.org/10.1016/j.jclepro.2017.02.043
36. Lima GR, Monteiro WF, Ligabue R, Santana RMC (2017) Titanate nanotubes as new nanostructured catalyst for depolymerization of PET by glycolysis reaction. Mater Res 20:588–595. https://doi.org/10.1590/1980-5373-mr-2017-0645
37. Kasuga T, Hiramatsu M, Hoson A et al (1998) Formation of titanium oxide nanotube. Langmuir 14:3160–3163. https://doi.org/10.1021/la9713816
38. Monteiro WF, dos Santos CAB, Einloft S et al (2016) Preparation of modified titanate nanotubes and its application in polyurethane nanocomposites. Macromol Symp 368:93–97. https://doi.org/10.1002/masy.201500146
39. Al-Sabagh AM, Yehia FZ, Eissa AMF et al (2014) Cu- and Zn-acetate-containing ionic liquids as catalysts for the glycolysis of poly(ethylene terephthalate). Polym Degrad Stab 110:364–377. https://doi.org/10.1016/j.polymdegradstab.2014.10.005
40. Geng Y, Dong T, Fang P et al (2015) Fast and effective glycolysis of poly(ethylene terephthalate) catalyzed by polyoxometalate. Polym Degrad Stab 117:30–36. https://doi.org/10.1016/j.polymdegradstab.2015.03.019
41. Lin Q, Gu Y, Chen D (2013) Attapulgite-supported aluminum oxide hydroxide catalyst for synthesis of poly(ethylene terephthalate). J Appl Polym Sci 129:2571–2579. https://doi.org/10.1002/app.38973
42. López-Fonseca R, Duque-Ingunza I, de Rivas B et al (2011) Kinetics of catalytic glycolysis of PET wastes with sodium carbonate. Chem Eng J 168:312–320. https://doi.org/10.1016/j.cej.2011.01.031
43. Syariffuddeen AA, Norhafizah A, Salmiaton AA (2012) Glycolysis of poly (ethylene terephthalate) (PET) waste under conventional convection-conductive glycolysis. Int J Eng Res Technol 1:1–8
44. Rostamizadeh M, Jafarizad A, Gharibian S (2018) High efficient decolorization of Reactive Red 120 azo dye over reusable Fe-ZSM-5 nanocatalyst in electro-Fenton reaction. Sep Purif Technol 192:340–347. https://doi.org/10.1016/j.seppur.2017.10.041
45. Goje AS, Mishra S (2003) Chemical kinetics, simulation, and thermodynamics of glycolytic depolymerization of poly(ethylene terephthalate) waste with catalyst optimization for recycling of value added monomeric products. Macromol Mater Eng 288:326–336. https://doi.org/10.1002/mame.200390034
46. Yue QF, Wang CX, Zhang LN et al (2011) Glycolysis of poly(ethylene terephthalate) (PET) using basic ionic liquids as catalysts. Polym Degrad Stab 96:399–403. https://doi.org/10.1016/j.polymdegradstab.2010.12.020
47. Awaja F, Pavel D (2005) Recycling of PET. Eur Polym J 41:1453–1477. https://doi.org/10.1016/j.eurpolymj.2005.02.005
48. Chen CH (2003) Study of glycolysis of poly(ethylene terephthalate) recycled from postconsumer soft-drink bottles. III. Further investigation. J Appl Polym Sci 87:2004–2010. https://doi.org/10.1002/app.11694
49. Wang S, Wang C, Wang H et al (2015) Sodium titanium tris(glycolate) as a catalyst for the chemical recycling of poly(ethylene terephthalate) via glycolysis and repolycondensation. Polym Degrad Stab 114:105–114. https://doi.org/10.1016/j.polymdegradstab.2015.02.006
50. Tsai CC, Chen LC, Yeh TF, Teng H (2013) In situ Sn^{2+}-incorporation synthesis of titanate nanotubes for photocatalytic dye degradation under visible light illumination. J Alloys Compd 546:95–101. https://doi.org/10.1016/j.jallcom.2012.08.081
51. Sim S, Cho EB, Chatterjee S (2016) H_2 and CO_2 uptake for hydrogen titanate ($H_2Ti_3O_7$) nanotubes and nanorods at ambient temperature and pressure. Chem Eng J 303:64–72. https://doi.org/10.1016/j.cej.2016.05.099
52. Sandoval A, Hernández-Ventura C, Klimova TE (2017) Titanate nanotubes for removal of methylene blue dye by combined adsorption and photocatalysis. Fuel 198:22–30. https://doi.org/10.1016/j.fuel.2016.11.007
53. Santos SRA, Jardim IS, Bicalho HA et al (2016) Multifunctional catalysts based on carbon nanotubes and titanate nanotubes for oxidation of organic compounds in biphasic systems. J Colloid Interface Sci 483:211–219. https://doi.org/10.1016/j.jcis.2016.08.025
54. Viana BC, Ferreira OP, Filho AGS et al (2011) Alkali metal intercalated titanate nanotubes: a vibrational spectroscopy study. Vib Spectrosc 55:183–187. https://doi.org/10.1016/j.vibspec.2010.11.007
55. Gomes IS, de Carvalho DC, Oliveira AC et al (2018) On the reasons for deactivation of titanate nanotubes with metals catalysts in the acetalization of glycerol with acetone. Chem Eng J 334:1927–1942. https://doi.org/10.1016/j.cej.2017.11.112
56. Turki A, Kochkar H, Guillard C et al (2013) Effect of Na content and thermal treatment of titanate nanotubes on the photocatalytic degradation of formic acid. Appl Catal B Environ 138–139:401–415. https://doi.org/10.1016/j.apcatb.2013.03.020
57. Chen A, Zhao T, Gao H et al (2016) Titanate nanotube-promoted chemical fixation of carbon dioxide to cyclic carbonate: a combined experimental and computational study. Catal Sci Technol 6:780–790. https://doi.org/10.1039/C5CY01024A
58. Wang H, Yan R, Li Z et al (2010) Fe-containing magnetic ionic liquid as an effective catalyst for the glycolysis of poly(ethylene terephthalate). Catal Commun 11:763–767. https://doi.org/10.1016/j.catcom.2010.02.011

Affiliations

G. R. Lima[1] · W. F. Monteiro[2] · C. M. Scheid[2] · R. A. Ligabue[2] · R. M. C. Santana[1]

[1] Graduate Program in Mining, Metallurgical and Materials Engineering, Federal University of Rio Grande do Sul, UFRGS, Porto Alegre, Brazil

[2] Graduate Program in Materials Engineering and Technology, Pontifical Catholic University of Rio Grande do Sul - PUCRS, Porto Alegre, Brazil